MEASUREMENT OF RELATIVE gf-VALUES AND COLLISIONAL DAMPING CONSTANTS FOR SPECTRAL LINES OF NEUTRAL CALCIUM

Thesis by

Kenneth Harold Olsen

In Partial Fulfillment of the Requirements

for the Degree of

Doctor of Philosophy

California Institute of Technology

Pasadena, California

1957

ACKNOWLEDGEMENTS

This research has been carried out under the supervision of Professor R. B. King, to whom I wish to express my gratitude for his encouragement, guidance, and helpful criticism throughout the course of the work. I also wish to thank Dr. P. M. Routly who gave invaluable assistance in constructing the furnace and in obtaining some of the spectrograms.

I appreciate the generous cooperation of the Mount Wilson Observatory for permitting me to use their laboratory for the experimental work.

ABSTRACT

The relative gf-values for 107 lines in 34 multiplets of Ca I between λ 2990 and λ 6720 have been derived from the photographic photometry of absorption lines excited in an electric furnace. All the lines arise from low terms whose excitation potentials range from 0.0 to 3.0 e.v.

A brief discussion of the method used for making the measurements is given, together with an outline of the theoretical relationships which are required to reduce the measurements to relative gf-values. The various components of the experimental apparatus are described in some detail.

In the second part, some preliminary studies have been made on the pressure broadening of Fe I and Ca I absorption lines in electric furnace spectrograms. By using relative gf-values for lines of these elements, empirical curves of growth have been constructed from which the collisional damping constants for some of the lines are derived. The experimental damping constants are compared with those calculated from the available theories of pressure broadening. The results indicate that observations of broadened absorption lines in furnace spectra may prove useful in determining collisional damping constants for many lines of astrophysical interest.

TABLE OF CONTENTS

PART ONE: MEASUREMENT OF RELATIVE gf-VALUES FOR SPECTRAL LINES OF NEUTRAL CALCIUM.

PART TWO: A PRELIMINARY STUDY OF PRESSURE EFFECTS IN ELECTRIC FURNACE SPECTRA.

LIST OF TABLES

LIST OF FIGURES

PART ONE

MEASUREMENT OF RELATIVE gf-VALUES FOR SPECTRAL LINES OF NEUTRAL CALCIUM

I. INTRODUCTION

The intensities of spectral lines are of considerable interest to astrophysicists engaged in the study of stellar atmospheres. In order to obtain quantitative information from intensity measurements on stellar spectral lines, it is often necessary to know the transition probabilities for the atomic lines in question. This report deals with the experimental study of the relative transition probabilities for some of the spectral lines of neutral calcium.

In principle, the transition probabilities for lines of a given spectrum may be calculated by means of quantum theory. Exact calculations have been made for the atomic hydrogen lines while a few other atoms, such as helium, have been treated by approximate methods. For complex spectra, our knowledge of atomic wave functions is at present limited, and also, computational difficulties make a theoretical treatment on a large scale impractical. Laboratory line intensity measurements from which the transition probabilities may be obtained are thus required in order to provide these important astrophysical data.

There are several ways of expressing transition probabilities for atomic transitions. The laws of quantum mechanics state that the transition probability is proportional to the square of the dipole matrix element between the two states involved. Other means of specification include: the emission intensity; the phenomenological A and B coefficients of Einstein; the "Line Strength", S, introduced by Condon and Shortley; and the f-value or "oscillator strength" as it is sometimes called. The interrelationships between these quantities are given in several textbooks such as those by Condon and Shortley[1], Aller[2],

and Unsold.[3] Because of its symmetry in the initial and final levels, Condon and Shortley's S notation has some advantages over the others, especially for theoretical work. However, the f-value notation has been used widely, particularly in astronomy, and this specification has been adopted in the present investigation.

The definition of the f-value originally was based on the classical electron theory of Lorentz. In this theory, the optical properties of a gas consisting of N atoms per unit volume were described in terms of the properties of n quasi-elastically bound electrons per unit volume. The ratio n/N was found to be constant for a given spectral line and was denoted by the dimensionless number, f. Thus, the f-value of a given line was regarded as a measure of the degree to which the atom behaved as a classically oscillating electron when it emitted or absorbed this line, and the term "oscillator strength" was applied to the f-value. A comparison of the classical electron theory with the quantum theory of matter later led to the correlation between the f-value and the matrix element.

A variety of experimental methods for determining f-values have been discussed in detail by Mitchell and Zemansky.[4] Shorter discussions are also given by Korff and Briet[5] and by Unsold.[3] These methods may be classified roughly as follows: a) emission; b) absorption; c) dispersion; d) depolarization; e) methods involving magneto-rotation; f) direct lifetime measurements for excited states. An absorption method was chosen for the present investigation.

Although absolute f-values are of great interest, much information may be obtained from a knowledge of relative f-values for lines in a given spectrum. In addition, once relative f-values are known, the entire

set can be placed on an absolute scale by a determination of the absolute value for one of the lines. The work discussed in this report employs a technique for the determination of relative f-values originally developed by R. B. King and A. S. King[6] which is most suitable for absorption lines arising from the low lying states of neutral metal atoms. Several investigators have successfully applied the method to the spectrum of iron[6], titanium[7],[8], vanadium[9], nickel[10], chromium[11], and cobalt.[12]

Most of the important calcium lines have been identified and the analysis of the spectrum is fairly complete. However, except for visual estimates, quantitative intensity measurements have been made for only a few of the lines.[13],[14],[15] Because of the astrophysical importance of this element, the present study was undertaken in order to provide more complete information on the calcium lines. In view of the fact that Dr. L. C. Green[16] and others are now engaged in determining wave functions for atomic states, it is hoped that the results of this investigation may also prove useful in testing the theoretical calculations.

II. REVIEW OF THEORY

In this section, the theoretical relationships which are needed for the reduction of the experimental data will be briefly discussed. More complete derivations and discussions are to be found in the books by Aller[2] and by Unsold.[3]

A. The Atomic Absorption Coefficient.

Classically, anomalous dispersion and line absorption may be regarded as arising from the resonance effects of the elastically bound electrons of a gaseous medium when it is subject to interaction with light waves. For an elastically bound electron in an atom subject to radiation losses and set into oscillation by the harmonic electric field of the radiation, the equation of motion may be set up and solved to give the amplitude and phase of the resulting steady state vibration. The oscillating electric field of the radiation tends to induce a dipole in the atom. If this atom is considered to be part of an isotropic, polarizable medium, the formulae of classical electricity and magnetism enable one to derive an expression for the dielectric constant of the medium which in turn is related to the index of refraction. This index is found to be complex which means, physically, that the medium not only refracts light but absorbs it as well. The complex refractive index may be separated into a real part which represents the ordinary refractive index, and into an imaginary part which represents the absorptivity. The absorptivity is a maximum at the resonance frequency, whereas the value of $n - 1$, where n is the ordinary refractive index, undergoes a change in sign at the resonance frequency. This behavior of n is commonly referred to as anomalous dispersion.

A rigorous expression for frequency dependence of the line absorption coefficient may be derived by the methods of quantum mechanics. Since most excited states of atoms have fairly short lifetimes, the Heisenberg uncertainty principle requires that there be an uncertainty, ΔE, in the energy of the atom in such a state. In other words, the state is not infinitely sharp; the uncertainty in energy being inversely proportional to the lifetime. Weisskopf and Wigner have derived a probability law giving the relative proportion of atoms in a small energy range, E to E + dE, in a broadened state of mean energy E_j. Considering two such broadened states having mean energies E_j and E_i between which transitions can occur, the principle of detailed balancing allows one to derive an expression for the atomic line absorption coefficient. For an atom at rest, the result of such a computation can be written in the form

$$\alpha_\nu = \frac{\pi e^2}{mc} f \frac{\Gamma}{4\pi^2} \frac{1}{(\nu_o - \nu)^2 + (\Gamma/4\pi)^2} \qquad (1)$$

α_ν is the absorption coefficient per atom at frequency ν in unit frequency interval, e and m are the electronic charge and mass, c is the velocity of light, and ν_o is the frequency given by the difference of E_j and E_i divided by Planck's constant. The transition probability for the line is expressed as the f-value. The natural damping constant, Γ, is proportional to the sum of the reciprocals of the lifetimes for the two states involved in the transition.

The classical theory also yields an expression for α_ν of the same form as equation 1 but with two important differences. The f-value is

missing since for a single oscillator it is assumed to be unity, and Γ has a different meaning. The classical damping constant is related to the mean rate of radiation of the oscillator and varies only with the frequency of the incident radiation.

Under certain conditions, the collisional processes which can broaden a spectral line may be treated within the framework of equation 1 by a suitable definition of a damping constant for these processes. The collisional and natural damping constants are additive.

In addition to the natural widths of spectral lines and to the widths arising from collisional processes, there is also a broadening of the lines due to kinetic motions of the atoms. This is known as Doppler broadening. An atom having a velocity v toward the observer will radiate or absorb a line centered on a frequency $\nu' = \nu_o(1 + v/c)$. The total α_ν is then obtained by averaging over all possible velocities. For a gas of molecular weight, M, at an absolute temperature, T, the fraction of atoms, dN/N, having velocities in the range v to v + dv is given by the Maxwellian velocity distribution:

$$\frac{dN}{N} = \sqrt{\frac{M}{2\pi RT}} \exp\left(-\frac{Mv^2}{2RT}\right) dv$$

where R is the gas constant per mole. Integrating over all velocities in the line of sight, the absorption coefficient at frequency ν becomes

$$\alpha_\nu = \frac{\pi e^2 f}{mc} \frac{\Gamma}{4\pi^2} \int_{-\infty}^{+\infty} \frac{\sqrt{M/2\pi RT}\, \exp\left(-Mv^2/2RT\right) dv}{(\nu_o + \nu_o v/c - \nu)^2 + (\Gamma/4\pi)^2} \quad . \qquad (2)$$

It is convenient to transform this integral by defining the following

quantities:

$$\Delta\nu_D = \frac{\nu_o}{c}\sqrt{\frac{2RT}{M}} \quad ; \text{ the "Doppler width" in frequency units}$$

$$\Delta\nu = \frac{\nu_o v}{c}$$

$$y = \frac{\Delta\nu}{\Delta\nu_D}$$

$$u = \frac{(\nu - \nu_o)}{\Delta\nu_D}$$

$$a = \frac{\Gamma}{4\pi\Delta\nu_D}$$

The integral becomes

$$\frac{\alpha_\nu}{\alpha_o} = H(a,u) = \frac{a}{\pi}\int_{-\infty}^{+\infty} \frac{\exp(-y^2)\,dy}{a^2 + (u - y)^2} \quad , \qquad (3)$$

where

$$\alpha_o = \frac{\pi e^2 f}{mc}\,\frac{1}{\Delta\nu_D\sqrt{\pi}} \, .$$

At a fixed temperature and pressure, a is constant for a given line and the integration may be performed over y. In general, H(a,u) cannot be expressed in closed form; asymptotic expansions and numerical methods must be used. Penner and Kavanagh[17] have reviewed the series expansions used by a number of investigators, while Mitchell and Zemansky[4], Hjerting[18], and Harris[19], have given helpful numerical tables for the evaluation of H(a,u).

B. The Curve of Growth.

In the present experiment, absorption lines are formed when light from a source of continuous radiation is passed through a column of vapor

containing the atoms whose absorption spectrum is desired. If light of intensity $I_{\nu,o}$ is incident on the column of vapor, the emergent intensity I_ν is given by

$$I_\nu = I_{\nu,o} \exp(-\tau_\nu) . \tag{4}$$

The optical depth, τ_ν, for this experiment is given by

$$\tau_\nu = Nh\alpha_\nu = Nh\alpha_o H(a,u)$$

where h is the length of the absorbing column, N is the number of atoms per unit volume which are effective in producing the line, and α_ν is the atomic absorption coefficient discussed in part A. The <u>profile</u> of the absorption line is defined by

$$1 - r_\nu = 1 - \frac{I_\nu}{I_{\nu,o}} = 1 - \exp(-Nh\alpha_\nu). \tag{5}$$

In practice, the finite slit width of the spectrograph and the imperfect resolution of the grating redistribute the energy incident on the spectrograph slit and constitute sources of instrumental broadening. The <u>observed</u> profile can be computed from an integral involving the theoretical line profile of equation 5 and the instrumental smoothing function. Unsold[3] has shown that in the absence of any scattered light arising from the optical elements of the apparatus, the ratio of the total energy absorbed by the line to the incident energy is not changed by instrumental effects. This ratio is defined as the <u>total absorption</u> or "<u>equivalent width</u>" of the line. The equivalent width in frequency units, W_ν, may then be written as

$$W_\nu = \int (1 - r_\nu)\, d\nu \ , \tag{6}$$

where the integral is extended over the line. For well separated lines, the limits of integration may be extended to $\pm\infty$, since contributions from other lines will be negligible in the region of interest. Introducing the Doppler width, $\Delta\nu_D$, equation 6 may be written in the form:

$$\frac{W_\nu}{\Delta\nu_D} = \int_{-\infty}^{+\infty} \left\{1 - \exp[-Nh\alpha_o H(a,u)]\right\} du \ . \qquad (7)$$

Equation 7 is the functional relationship between the total absorption and the number of atoms active in absorbing the line and gives the so-called "curve of growth" for the line.

The curve of growth is an important tool in astrophysics, where an equation similar to 7, but modified in accordance with a model adopted for the structure of the stellar atmosphere, is used to obtain information on temperatures, pressures, turbulence and abundances in stellar atmospheres. Equation 7 strictly applies to the laboratory absorption tube experiment where the temperature, pressure, and concentration throughout the column of absorbing vapor are constant.

With grating spectrograms, it is convenient to measure the equivalent width in wavelength units rather than in frequency units. If W_λ and $\Delta\lambda_D$ are the equivalent width and Doppler width in wavelength units, then $W_\lambda/\Delta\lambda_D = W_\nu/\Delta\nu_D$ and $\Delta\lambda_D = (\lambda_o/c)\sqrt{2RT/M}$, where λ_o is the wavelength at the center of the line. Defining a quantity, X, such that

$$X = Nh\alpha_o = Nhf \frac{\pi e^2 \lambda_o^2}{mc^2 \Delta\lambda_D \sqrt{\pi}} , \qquad (8)$$

equation 7 becomes

$$W_\lambda / \Delta\lambda_D = \int_{-\infty}^{+\infty} \left\{1 - \exp[-XH(a,u)]\right\} du. \qquad (9)$$

Two special cases of equation 9 are of interest.

Case a. Pure Doppler broadening: In this case $a \to 0$, $H(a,u)$ becomes $\exp(-u^2)$ and the integrand in equation 9 may be expanded in a series and integrated term by term to give

$$\frac{W_\lambda}{\Delta\lambda_D} = \sqrt{\pi} \sum_{n=1}^{\infty} \frac{X^n (-1)^{n+1}}{n! \sqrt{n}} \quad . \tag{10}$$

Note that for $X \ll 1$,

$$\frac{W_\lambda}{\Delta\lambda_D} = \sqrt{\pi} X \quad \text{or} \quad W_\lambda = \frac{\pi e^2 \lambda_o^2}{mc^2} Nfh \quad , \tag{11}$$

and the total absorption increases linearly with Nf. For $X \gg 1$, Unsold gives the following asymptotic expansion:

$$\frac{W_\lambda}{\Delta\lambda_D} = 2\sqrt{\ln X}\left\{1 + \frac{0.2886}{\ln X} - \frac{0.1355}{(\ln X)^2} + \cdots\right\} \tag{12}$$

Case b. Damping predominant: Here $H(a,u)$ becomes $a/\sqrt{\pi}\, u^2$, and for large X the integration gives

$$\frac{W_\lambda}{\Delta\lambda_D} = 2\sqrt{\sqrt{\pi}\, aX} \quad , \tag{13}$$

that is, the equivalent width increases as $\sqrt{Nf\Gamma}$. For intermediate values of X, numerical tables must be used to evaluate equation 9.

Figure 1 gives a plot of $\log (W_\lambda/\Delta\lambda_D)$ versus $\log \frac{Nhf}{2\pi\Delta\nu_D}$ $[=\log(10.6X)]$ for various values of the damping parameter, a. It illustrates the approximately linear relationship between $W_\lambda/\Delta\lambda_D$ and X for small $W_\lambda/\Delta\lambda_D$. This is the region where the shape of the absorption coefficient is de-

termined primarily by Doppler broadening. As Nf is increased, the curves enter an intermediate region where both Doppler and damping effects contribute; soon damping takes over completely and the equivalent width increases as $\sqrt{Nf}$. At a given value of Nf, the relative importance of damping and Doppler broadening is determined by the parameter a.

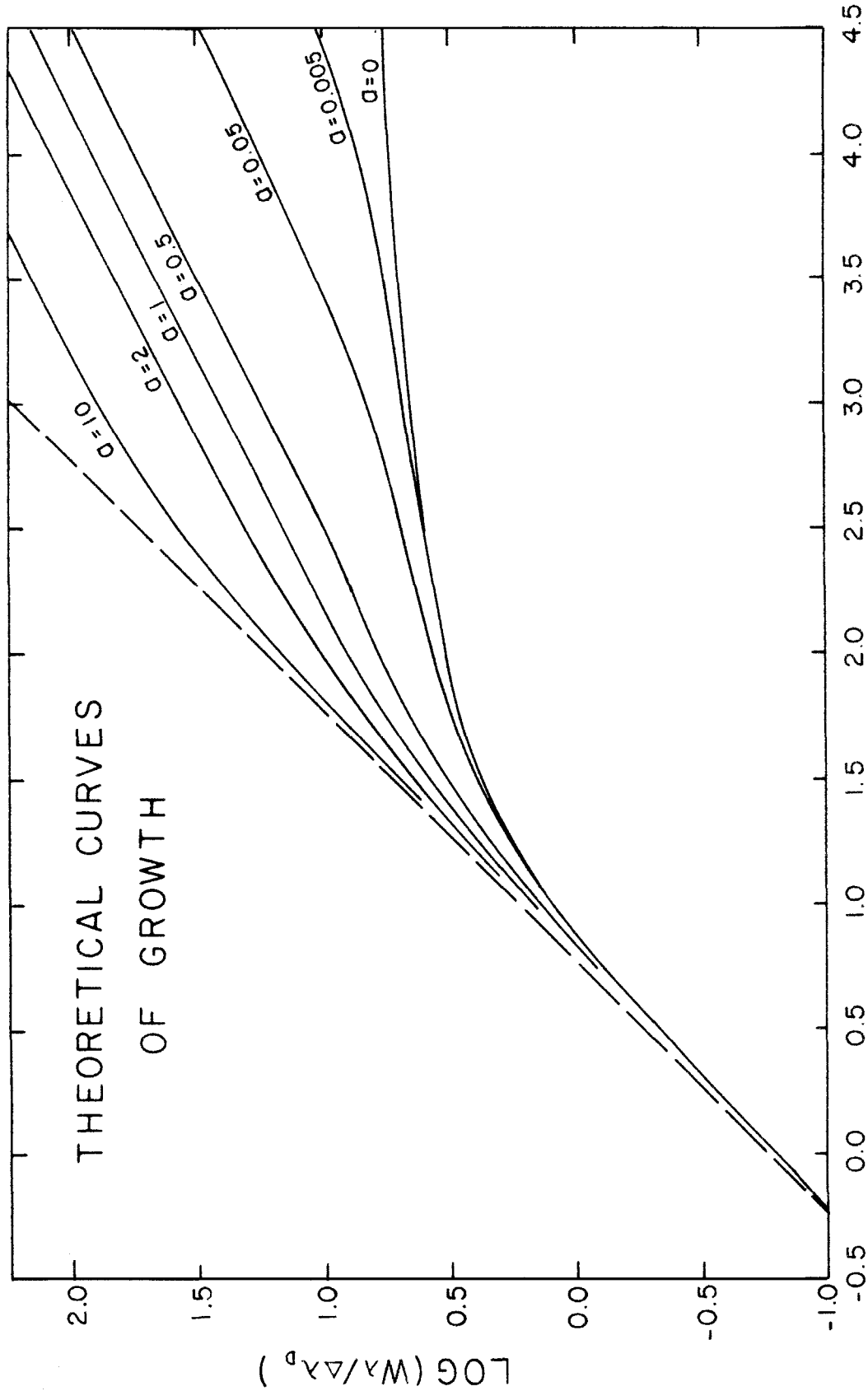
THEORETICAL CURVES
OF GROWTH
a=10
a=2
a=1
a=0.5
a=0.05
a=0.005
a=0
LOG (Wλ/Δλb)
LOG (Nfh/2πΔυD)
2.0
1.5
1.0
0.5
0.0
-0.5
-1.0
-0.5
0.0
0.5
1.0
1.5
2.0
2.5
3.0
3.5
4.0
4.5

FIGURE 1

III. METHOD

The experimental method for determining relative f-values consisted of measuring the equivalent widths of those CaI absorption lines which were weak enough to be on or near the linear portion of the curve of growth. Doppler widths and the relative concentrations of active atoms in the different atomic energy levels were computed from observed furnace temperatures. The curves of growth discussed in the previous section were then used to calculate the corresponding relative f-values.

A beam of light from a lamp giving a continuous spectrum was passed through an electric resistance furnace in which the calcium sample had been vaporized. This furnace employed a graphite tube heated to the desired temperature by means of a large electric current at low voltage. The resulting absorption lines were photographed with a high dispersion spectrograph of the Rowland type. The plates were traced with a recording microphotometer and the equivalent widths were measured from these tracings.

King and King[6] have shown that a condition of thermodynamic equilibrium exists in the furnace tube. The relative populations of atoms in the different lower energy levels from which the lines arise can therefore be computed with the aid of the Boltzmann relation:

$$\frac{N_i}{N_o} = \frac{g_i}{g_o} \exp\left(-\frac{E_i}{kT}\right) \qquad (14)$$

where N_i and N_o are, respectively, the number of atoms in the excited state, i, and the number in the ground state, o; g_i and g_o are the statis-

tical weights, $2J + 1$, of these states; E_i is the excitation potential of the ith state; k is the Boltzmann constant. Multiplying equation 14 through by f_i and rearranging gives:

$$g_i f_i = \frac{g_o}{N_o} N_i f_i \exp(+\frac{E_i}{kT}) \quad . \tag{15}$$

Values of E_i were obtained from the data on atomic energy levels compiled by Moore.[20]

For a given exposure, a value of X for each equivalent width was read from the curve of growth. Combining equations 8 and 15 gave relative values of $Kgf\lambda$ for the lines. K is a scale factor for a given exposure and is proportional to the amount of calcium vapor in the furnace. Relative gf-values for all the lines were then placed on a common scale by adjusting the value of K for each exposure. Since gf-values are often used directly in astrophysical applications, a tabulation of the relative gf-values is often more convenient than one of f-values. The results reported here are given in terms of the gf-values.

At the temperatures and pressures used in this investigation, the contributions of natural and collisional damping to the line broadening were negligible. Therefore, the curve of growth for pure Doppler broadening ($a = 0$) was used for reducing the observations. Mr. Max Seamons of the Jet Propulsion Laboratory programed equation 10 for the Datatron computer and the results were arranged in the form of a table giving X as a function of $W_\lambda/\Delta\lambda_D$. The difficulty of obtaining reliable equivalent widths for very weak lines and the relative "flatness" of the curve for $\log (W_\lambda/\Delta\lambda_D) > 0.3$ limited the usable range of equivalent width values

from any single exposure. This range amounted to about a factor of ten. A "step-down" technique for comparing larger ranges in intensity was carried out by varying the amount of vaporized sample. This made it possible to bring different sets of lines within the usable region of the curve of growth. At the higher vapor densities, the intrinsically weak lines were observed in this region, while successively stronger lines appeared as the concentration of absorbing vapor was decreased. Because the concentration of absorbing atoms was different for each exposure, the scale of gf-values measured on successive exposures was also different. The results from a series of exposures were then combined on a single scale by determining the scale factors from the gf-value measurements for lines appearing in common on exposures taken at slightly different vapor densities.

A much larger range of intensities may be directly compared by using the square root portions of the curves of growth. Unfortunately, this requires more information on the magnitudes of the damping constants than is presently known. Theoretical considerations lead one to expect that all multiplets may not have the same damping factor under the physical conditions existing in the furnace. At present it seems best to use the procedure outlined above for relative gf-value measurements.

The methods of measuring equivalent widths from microphotometer tracings have been discussed in detail in a thesis by Hill.[21] The same procedure has been used here except that only the weakest lines were treated as triangles. Profiles of stronger lines were broken up into a number of horizontal segments which were then summed to give the equivalent widths.

The absorption method outlined here has the advantage of simplicity with respect to both apparatus and theory. Accurate temperature readings are required because of the critical manner in which the Boltzmann factors affect the relative populations of the atoms in the various energy levels. When used with this type of furnace, the optical pyrometer provides temperatures accurate to a fraction of a per cent.

As stated above, one disadvantage of the absorption method used in this work is the limited range of intensities which may be compared directly on a single spectrogram since the "step-down" technique increases the possibility of introducing errors into the final results. The outstanding disadvantage of the method is the error in equivalent width measurements caused by the grain irregularities of the photographic emulsion. This grain "noise" is superimposed on all line profiles but introduces proportionately greater errors for the weaker lines. Because this grain effect is random in operation, a large number of independent exposures are required in order to minimize it. A compromise must be reached between the desired accuracy and the amount of time spent in reducing a very large number of measurements.

In spite of the disadvantage of photographic photometry, it was used in preference to a photoelectric technique for measuring the equivalent widths. Photoelectric methods are most suitable for emission line studies and become somewhat complicated for the photometry of weak absorption lines. It was desirable to study the lines in absorption rather than in emission because the corrections for the self absorption and the self reversal of emission lines are often difficult to evaluate.

Other possible sources of error, both random and systematic, are

summarized by King and King[6] and by Hill.[21] Some of these will be discussed in following sections of this thesis.

IV. APPARATUS

A. The Furnace

The furnace used in this investigation is a modification of the large hood furnace designed by A. S. King[22] and is located at the Pasadena Laboratory of the Mount Wilson Observatory. The heating element is a graphite tube 12 inches long, 0.50 inches I.D. and 0.75 inches O.D. The tube is held at each end by a split cylindrical block of graphite 3.75 inches in diameter and 3 inches long. These blocks are in turn held by water cooled electrodes of cast bronze. Concentric with the graphite tube are two molybdenum radiation shields and a large brass water jacket. This assembly rests on a steel base plate through which pass the connections for the current conductors, water lines, and the vacuum line. The entire structure is enclosed by a large forged steel hood provided with two quartz windows opposite the ends of the graphite tube. An air tight seal between the base plate and hood is achieved by means of a rubber gasket.

Electrical power for the furnace is supplied by a heavy duty transformer capable of giving over 2000 amperes of 60 cycle a.c. A bank of switches enables one to adjust the furnace input voltage in 5 volt steps from 5 volts to 50 volts. Fine adjustment within each range is provided by means of a motor driven voltage control. Temperatures up to about 2800° C. are obtainable with this arrangement. Power requirements for the higher temperatures may be decreased by using graphite tubes whose wall thickness have been reduced by about 0.010 inch.

Unlike the metals such as iron, cobalt and nickel which have been

previously studied in this type of furnace, calcium presented a special problem. The boiling point of calcium is 1240° C, whereas the boiling points for Fe, Ti, V, Ni and Co are of the order of 3000° C. Temperatures in excess of 2000° C were required to observe these absorption lines arising from states with excitation potentials above 2 e.v., and under these conditions, calcium had a relatively high vapor pressure. The rate at which the sample was lost could be considerably reduced by requiring the furnace to be vacuum tight and to be isolated from the pumping system during a run. Tests showed that the furnace had a leak rate of about 2 microns per minute at the lowest pressure (5 microns) obtainable with a Cenco Hypervac pump and therefore proved to be well adapted to this technique. After isolating the pump from the furnace by means of a vacuum valve, the furnace was usually operated with an atmosphere of about 0.5 to 1 cm. of helium. A pressure rise of the order of 2 cm. was noted during runs and was probably caused by outgassing of the large graphite electrode clamps during heating.

Electrolytically purified calcium metal was used for most of the samples. This was cut into small pieces and was placed in the tube with a charging spatula. It was necessary to recharge the tube after about an hour of continuous furnace operation. Molecular bands identified as the strongest absorption bands of CaCl, CaF and CaH were observed in the red region of the spectrum (5900-7000 Å). It was found that the CaCl and CaF impurities could be eliminated by using dried, chemically pure CaO powder but that the CaH bands remained. The CaH bands (6700-7000 Å) gave a bright red color to the vapor and indicated roughly the amount of vaporized calcium in the tube. The CaO powder was also more

stable and showed less bubbling at high temperatures than did calcium metal, but the higher vapor density provided by the metal samples was required in order to observe the weaker lines.

B. The Light Source and Optical System

The source used for the continuous spectrum was a 250 watt high pressure Xenon discharge lamp manufactured in Germany by Osram. The lamp consists of two conical tungsten electrodes enclosed in a quartz bulb and operates on 220 volts a.c. The lamp is provided with a starting apparatus which gives a 20,000 volt pulse to initiate the discharge. The bulb operates in a vertical position and is air cooled. The very bright spot appearing near the lower electrode was imaged on the spectrograph slit after its light had passed through the furnace tube. This source gave an excellent continuum for absorption line studies as its color temperature is well in excess of 3000° K. The high radiance of the spot permitted the use of exposure times less than 30 seconds, thus minimizing errors due to the slight fluctuation in furnace temperature and the changing concentration of calcium vapor which may occur during an exposure.

Tests with the lamp revealed a very smooth continuum with only a few diffuse emission lines in the region λ 2600 Å to λ 8000 Å. The main objection to this source was the erratic wandering of the bright spot over the pointed electrode surface. As the brightest region of the spot is only a fraction of a millimeter in diameter, this wandering sometimes caused the image of the spot to move off the spectrograph slit for short periods, and exposures of the correct density could consistently be obtained only by using exposure times greater than about

10 seconds. Exposure times between 10 and 30 seconds were used for most of the plates.

The optical system consisted of three lenses and one prism, all of fused quartz. Since the light beam from the Xenon lamp passed through the furnace in a horizontal direction, the prism was necessary in order to deflect the beam to the vertical direction that was required by the spectrograph mounting. The prism occupied a position about 50 cm. above the spectrograph slit. The focal lengths of the lenses were (1) 15 cm., (2) 50 cm., (3) 78 cm., and were placed as follows: Lens 1 imaged the bright spot of the Xenon lamp at the midpoint of the furnace tube which was 80 cm. from the lamp. The light from this image was received by lens 2 and rendered parallel. Lens 3 intercepted this parallel beam and formed an image of the spot on the slit. The aperatures were sufficient to provide uniform illumination over the ruled surface of the grating.

C. The Spectrograph

The spectrograph used was the 15-foot vertical Rowland spectrograph at the Mount Wilson Observatory. Its dispersion in the first order is 3.730 Å/mm. The plate holder is made to receive a plate approximately 2 inches wide by 18 inches long, so that in the first order, a wave length interval of 1700 Å may be recorded on a single exposure. Fine grain, high contrast plates were used to record the absorption lines. Eight to nine exposures, each approximately 2 mm. wide and separated by clear spaces of about the same distance, were recorded on a single plate. A slit width of approximately 0.020 mm. was used for most of the exposures.

The plates were calibrated by imaging the light from a voltage stabilized Phillips ribbon filament lamp onto a step slit mounted in place of the spectrograph slit. The calibration plates gave a series of exposures (usually ten) of differing degrees of blackening which could then be translated into relative intensities by means of the known step slit openings. Calibration plates were of the same stock as the spectrum plates and were exposed for the same length of time. The calibration and spectrum plates were developed simultaneously in D-19 developer for 4 minutes.

For each of the successive step slit exposures, it was necessary to maintain the same exposure time to within a fraction of a second. In view of the short exposure times used, deviations larger than this would cause appreciable errors in the plate calibration curves. Manual timing of the exposures was felt to be unsatisfactory, and so a device was assembled which operated the shutter automatically. This assembly consisted of a solenoid operated Packard shutter clamped about 2 inches above the slit. Current to the solenoid was controlled by means of a photographic timer manufactured by the Industrial Timer Corporation. The timer was essentially a synchronous clock motor which actuated a microswitch in the solenoid circuit. Exposure times ranging from 1 to 60 seconds could be chosen by setting the dial — the timer automatically resetting itself after each cycle. Tests showed that the variation in successive exposure times was less than 0.2 seconds.

As mentioned in section II, scattered light in the spectrograph tends to fill in the absorption lines, resulting in equivalent widths that are systematically too small. A test was made to determine the

magnitude of this scattered light by using low contrast Eastman 103-0 plates whose latitude was further increased by short development in Eastman D-76 developer. The test was made in the second order in the wavelength interval λ 2450 Å - λ 3300 Å. With the light source focused on the spectrograph slit, two 30 second exposures were taken. The first recorded the dispersed plus scattered light contributions. A filter which cut off all light below λ 4200 Å was then placed over the slit and a second exposure recorded only the scattered light. A calibration plate was developed with this plate and density measurements were made with a Beckman Model B densitometer. The two exposures showed an intensity ratio of 0.01. This ratio represents a minimum value for the scattered light, since the test does not record the scattered light due to wavelengths below 4200 Å. Because the lamp intensity decreases with wavelength, the contribution of scattered light could reasonably be taken as less than about 3 % of the dispersed light. With this relatively small contribution, it was felt that correction of the observed profiles for scattered light was unnecessary.

D. The Optical Pyrometer

The temperatures of the furnace tubes were read with a Leeds and Northrup optical pyrometer, model 8622-C. This pyrometer was checked against a standard instrument at the Leeds and Northrup agency in Los Angeles and the two were found to agree within the limits of reading error. A right angle prism inserted into the beam from the furnace allowed the temperature of the inner wall of the furnace tube to be read through one of the windows in the furnace hood. During a reading, a shield was placed over the other window to exclude the light from the Xenon lamp.

A correction for the light losses in the prism and window was required in order to obtain true furnace temperatures.

The optical pyrometer matches the intensity of a standard lamp filament contained in the pyrometer with the intensity of the luminous object whose temperature is desired. The observable wavelength interval is limited by means of a red filter, and the temperature scale is based on Wien's approximation to a black body energy distribution. Application of Wien's Law enables one to correct for readings made on non-black objects and for measurements obtained through slightly absorbing windows. The resulting correction formula may be written in the form:

$$\frac{1}{T} - \frac{1}{\theta} = A \qquad (16)$$

T is the true temperature of the object in degrees Kelvin; θ is the equivalent black body temperature and is indicated by the pyrometer scale. The negative constant, A, is a characteristic of the pyrometer and the associated optical elements. The window and prism corrections were obtained by observing the controlled ribbon filament lamp with and without the window and prism in the light path. From three to six successive pairs of readings were taken at each of eight different lamp currents. Equation 16 was then used to compute the value of A for each pair of readings. These A values were then averaged; the residuals of the individual determinations showed no systematic deviation from the assumed constancy of A. The mean value of A was then used to compute a correction curve which gave the additive corrections to be applied to the temperatures observed through the prism and window.

The xH scale (1500° - 2900° C) of the pyrometer was used almost exclusively for temperature measurements, and it was found that, with care, successive readings on this scale could be reproduced to within about 5° C. Although such deviations may in some cases affect the Boltzmann corrections by as much as 5%, such reading errors should in general be random in operation and should appear in the final results principally as an increase in the value of the probable error.

E. The Microphotometer

Most of the equivalent widths were measured from tracings made on the recording microphotometer located in the Robinson Astrophysical Laboratory of the California Institute of Technology. This machine uses a Leeds and Northrup Speedomax recorder to trace the absorption line profiles. A chart-to-plate magnification of 108 was used for tracing the absorption lines, whereas a magnification of 27 was employed for calibration plate tracings. Otherwise, the same settings were used for both spectrum and calibration plates. A slit length nearly equal to the width of the spectrum minimized the grain fluctuations.

The microphotometer originally designed by Dunham at the Mount Wilson Laboratory was used for some of the first plates obtained in the ultra violet region of the spectrum. The tracings from this instrument were made on strips of sensitized paper which required photographic processing. For subsequent work, tracings obtained with the microphotometer in the Robinson Laboratory were used in preference to those made with the Dunham instrument.

The main disadvantage of both the instruments discussed above is the time consuming procedure that is required to translate the tracings

into an intensity scale. The markings for each line profile must be read from the plate calibration curves before the equivalent widths may be calculated, and the possibility of introducing errors into the reductions is thereby increased.

Dr. Horace Babcock of the Observatory staff has developed a direct intensity microphotometer which is capable of giving excellent results. This instrument requires a specially prepared calibration wedge in which the intensity is a linear function of the distance along the plate. A device for preparing such wedges was constructed by Mr. B. R. Parnes and was given a thorough test by Dr. P. M. Routly and the writer. This calibration apparatus consists of a cardboard tube 9.5 feet long with internal diaphragms to minimize reflections from the tube walls. Light from a 900 watt projection bulb forms a small image on an opal glass diffusing screen at one end of the tube, and the light from this screen is photographed at the opposite end. Immediately in front of the photographic plate is a 10-inch diameter disk which revolves at about 3000 rpm. The revolving disk is machined so that the exposure time at the plate is a linear function of distance across the width of the plate. The proper spectral regions are selected by means of filters placed between the lamp and the diffusing screen.

The resulting wedges were tested against step slit calibrations made with the 15-foot spectrograph. The results of these tests showed that the two sets of calibration curves usually agreed reasonably well for a density range of from 50% to 90% blackening. Below 50%, the wedge calibrations showed more blackening for the same light intensity than did the step slit calibrations. Also, the variation in the slope of the characteristic curves with wavelength was masked in the wedges.

Although these difficulties could be overcome by building a considerably more elaborate wedge calibration device, the step slit calibrations were considered to be the best available at the time and were used in the reduction of all the tracings.

V. RESULTS

Relative gf-values were measured for 107 lines in 34 multiplets of the Ca I spectrum. The measured lines lie between λ 2990 Å and λ 6720 Å. They constitute 81% of those absorption lines listed in the Revised Multiplet Table[23] as arising from terms having excitation potentials less than 3 e.v. A total of 135 individual exposures appearing on 18 plates were photometered and reduced. Furnace temperatures for these exposures ranged from 1960° K to 2960° K.

The results of the measurements are given in Table 1 where the arrangement of lines within the multiplets follows the scheme of the Revised Multiplet Table. The first two columns of Table 1 give the multiplet number and the term designation for each of the multiplets. The third and fourth columns give the inner quantum numbers, J, and the wavelengths for the individual lines of the multiplets. The fifth column lists the common logarithms, on an arbitrary scale, of the means of the measured gf-values. The last column lists the number of individual measurements made on each line and these numbers are indicative of the relative weights which are to be assigned to the gf-value measurements. When the gf-values for all the lines in the multiplet have not been measured, an asterisk (*) follows the multiplet number.

The measurements for several of the lines may have been affected by the blending of the calcium line with a line of an impurity, such as iron or titanium. When there is some doubt that the measured strength was due entirely to the calcium line, the log gf-value is placed in parentheses in Table 1.

Because of the random errors in equivalent width measurements, the resulting individual gf-values showed considerable scatter about the

means. In most cases, the average deviations from the mean gf-values were found to be of the order of 15%.

It has been pointed out previously that in addition to the random errors of photographic photometry, there is the possibility for the introduction of systematic errors in reducing the measurements from different exposures to the same scale. The measurements covered wide ranges both in wavelength and in intensity. When possible, the scale factors for exposures covering overlapping wavelength and intensity ranges were determined by making ten or more measurements on each of five or more lines which were common to the two sets of exposures. Hence, systematic errors with respect to both wavelength and intensity should be less than the average deviations (15%) of the gf-value measurements.

The transition probabilities for lines in multiplets 1, 3, 4, 6, 9 and 10 have been obtained by Schuttevaer and his colleagues.[15] Schuttevaer's values were derived from photographic photometry of calcium emission lines in an arc spectrum. His measurements for these lines were compared with those found in the present investigation — the gf-values for the lines of multiplet number 3 being treated as the standards for the comparison. Schuttevaer's values for the lines of multiplets 4, 6, 9 and 10 were found to be from 20% to 35% lower than the values found in the present study -- the percentage differences being fairly consistent for all the lines of a given multiplet. His value for the intersystem line (multiplet number 1) is about <u>seven</u> times larger than the value found here. Although systematic errors with respect to both wavelength and intensity may be present in the data given in Table 1, the magnitudes of such errors should be less than the 15% mentioned previously.

The photographic photometry of emission lines requires that one accurately determine the wavelength variation of the plate sensitivity since any errors in the sensitivity calibration will have large effects on the measured intensities of the emission lines. Such a calibration is a difficult procedure, especially for a low dispersion prism spectrograph of the type used by Schuttevaer. In addition, Schuttevaer's measurements of the intensities of the lines of multiplet number 3 were complicated by the presence of molecular bands in this wavelength region. It seems likely that at least some of the discrepancy between the two sets of data for multiplets 3, 4, 6, 9 and 10 may be accounted for by the probable uncertainties in the emission line measurements. The question could be resolved by making measurements on calcium absorption lines using a high dispersion grating spectrograph of the Paschen-Runge type. This type of instrument can be provided with several plate holders so that exposures of lines in widely differing wavelength regions may be obtained simultaneously. This would eliminate the step-wise comparison of the lines in the different wavelength regions which was required by the Rowland spectrograph used in the present investigation.

Schuttevaer's result for the intersystem line (λ 6572) is certainly in error. This line was very weak on his plates and had to be compared with a weak, high level emission line in the ultraviolet region of the spectrum. Because the two lines differ considerably in excitation potential, the Boltzmann factor enters critically into the calculation of the relative transition probabilities. Measurements of the excitation temperatures for the arc are subject to large uncertainties, and it is reasonable to assume that Schuttevaer's large value for the relative transition probability of λ 6572 was primarily caused by an error

in his temperature measurements. In the present absorption study, the furnace temperatures were accurately known and the intersystem line was compared directly with the lines of multiplet number 3 and with the other lines in the red region.

The resonance line (λ 4226, multiplet number 2) was extremely strong in comparison with all the other lines listed in Table 1 and, therefore, its gf-value could not be measured by the present technique. However, the ratio of the f-values of λ 4226 and λ 6572 has been measured by Prokofjew.[13] This was done by using the so-called "hook" method. This "hook" method is one involving measurements of the anomalous dispersions of the lines and is capable of yielding quite accurate results. Prokofjew found a value of 3.3×10^4 for the ratio of the f-values of the resonance and intersystem lines, i.e.

$$\frac{f\ (\lambda\ 4226)}{f\ (\lambda\ 6572)} = 3.3 \times 10^4 \ .$$

No experimental measurements of the <u>absolute</u> f-values for any of the calcium lines have as yet been made. However, two theoretical calculations have been made for the absolute f-value of the resonance line. Hartree and Hartree[24] and Trefftz[25] computed wave functions for the states involved in the resonance transition and from these were able to derive an absolute f-value for λ 4226. Hartree and Hartree obtained a value of 2.27, whereas Trefftz's value was 1.46. Trefftz's calculation involved more elaborate wave functions than those used by Hartree and Hartree and is probably more reliable. If one assumes the value of 1.46 for the absolute f-value of λ 4226, together with Prokofjew's value of

3.3×10^4 for the ratio of the f-values of λ 4226 and λ 6572, then the gf-values given in Table 1 may be placed on an absolute scale. The factor by which the gf-values in Table 1 are to be multiplied to obtain absolute gf-values is then 1.65×10^{-5}. If the Hartree value for λ 4226 were correct, the factor would be 2.56×10^{-5}.

In conclusion, some possibilities for future experimental work on the intensities of the neutral calcium lines may be mentioned. First, since the theoretical f-values may be somewhat inaccurate, an experimental measurement of the absolute f-value for one of the lines should be attempted. Second, the relative gf-value measurements should be extended so as to include lines which arise from terms having low excitation potentials from 3.0 to 4.9 e.v. These high level lines were too weak to be detected by the present method, but their relative gf-values could be obtained by observations with a source having higher excitation temperatures than are possible with the King furnace.

TABLE 1

Relative gf-values for Lines of Ca I

Mult. No.	Designation	J	λ	log gf	No. Meas.
(1)	$4^1S - 4^3P^o$	0-1	6572.781	0.430	34
(3)	$4^3P^o - 5^3S$	2-1	6162.172	4.651	25
		1-1	6122.219	4.466	27
		0-1	6102.722	3.994	22
(4)	$4^3P^o - 4^3D$	2-3	4454.781	5.141	7
		1-2	4434.960	4.783	7
		0-1	4425.441	4.478	10
		2-2	4455.887	4.319	9
		1-1	4435.688	4.351	10
		2-1	4456.612	3.248	6
(5)	$4^3P^o - 4p^2\ ^3P$	2-2	4302.527	5.118	6
		1-1	4298.986	4.416	6
		2-1	4318.652	4.637	7
		1-0	4307.741	4.536	7
		1-2	4283.010	4.649	7
		0-1	4289.364	4.523	6
(6)	$4^3P^o - 6^3S$	2-1	3973.707	3.943	14
		1-1	3957.053	3.677	17
		0-1	3948.901	3.200	11
(9)	$4^3P^o - 5^3D$	2-3	3644.410	4.545	3
		1-2	3630.748	4.332	4
		0-1	3624.111	3.914	5
		2-2	3644.765	3.866	7
		1-1	3630.974	3.748	3
		2-1	3644.990	2.584	3
(10)	$4^3P^o - 7^3S$	2-1	3487.598	3.475	7
		1-1	3474.763	3.247	9
		0-1	3468.476	2.696	10
(11)*	$4^3P^o - 6^3D$	2-3	3361.918	4.297	5
		1-2	3350.209	4.004	4
		0-1	3344.513	3.706	11
		2-2	3362.131	3.658	11
		1-1	3350.361	3.624	5

Table 1 — continued

Mult. No.	Designation	J	λ	log gf	No. Meas.
(12)	$4^3P^o - 8^3S$	2-1	3286.067	3.255	12
		1-1	3274.661	3.009	13
		0-1	3269.090	2.503	7
(13)	$4^3P^o - 7^3D$	2-3	3225.896	4.089	7
		1-2	3215.145	3.779	7
		0-1	3209.930	3.374	9
		2-2	3226.129	3.337	11
		1-1	3215.334	3.221	5
(14)	$4^3P^o - 9^3S$	2-1	3180.521	2.962	14
		1-1	3169.854	2.796	12
		0-1	3164.618	2.236	3
(15)	$4^3P^o - 8^3D$	2-3	3150.738	3.792	7
		1-2	3140.782	3.395	10
		0-1	3136.003	3.102	13
		2-2	3151.280	2.975	12
		1-1	3141.164	2.967	10
(16)	$4^3P^o - 10^3S$	2-1	3117.656	2.713	11
		1-1	3107.388	2.486	5
		0-1	3102.36	(2.274)	2
(17)	$4^3P^o - 3d^2\ ^3P$	2-2	3006.858	4.500	7
		1-1	2999.641	3.900	8
		2-1	3009.205	4.056	7
		1-0	3000.863	(4.225)	2
		1-2	2997.309	4.093	8
		0-1	2994.958	4.010	9
(18)*	$3^3D - 3d4p\ ^3F^o$	3-4	6439.073	4.955	26
		2-3	6462.566	4.809	21
		1-2	6493.780	4.606	18
		3-3	6471.660	4.144	8
		2-2	6499.649	4.003	15
(19)*	$3^3D - 3d4p\ ^1D^o$	2-2	6455.600	3.500	9
		1-2	6449.810	4.215	9
(20)*	$3^3D - 5^3P^o$	3-2	6169.559	4.321	16
		2-1	6169.055	4.108	13
		1-0	6166.443	3.736	9
		2-2	6161.289	3.726	9
		1-1	6163.758	3.585	9

Table 1 — continued

Mult. No.	Designation	J	λ	log gf	No. Meas.
(21)	$3^3D - 3d4p\ ^3D^o$	3-3	5588.757	5.176	28
		2-2	5594.468	4.947	24
		1-1	5598.487	4.808	20
		3-2	5601.285	4.498	12
		2-1	5602.846	4.392	14
		2-3	5581.971	4.501	14
		1-2	5590.120	4.383	15
(22)	$3^3D - 3d4p\ ^3P^o$	3-2	5270.270	5.059	22
		2-1	5265.557	4.750	21
		1-0	5262.244	4.440	24
		2-2	5264.239	4.362	21
		1-1	5261.706	4.328	21
		1-2	5260.375	3.340	3
(23)*	$3^3D - 4^3F^o$	3-4	4585.871	4.620	12
		2-3	4581.402	4.482	9
		1-2	4578.558	4.197	8
(25)	$3^3D - 5^3F^o$	3-4	4098.533	4.307	11
		2-3	4094.930	4.154	10
		1-2	4092.633	4.006	9
(26)	$3^3D - 6^3F^o$	3-	3875.807	(4.095)	3
		2-	3872.552	(3.835)	3
		1-	3870.506	(3.750)	3
(27)*	$3^3D - 7^3F^o$	3-	3753.367	3.762	8
		2-	3750.349	3.614	7
(28)	$3^3D - 8^3F^o$	3-	3678.240	3.514	5
		2-	3675.307	3.387	4
		1-	3673.448	3.201	1
(32)	$3^1D - 3d4p\ ^1P^o$	2-1	6717.685	4.237	10
(33)	$3^1D - 3d4p\ ^1F^o$	2-3	5349.472	4.672	19
(34)	$3^1D - 5^1P^o$	2-1	5041.620	4.557	10
(35)	$3^1D - 4^1F^o$	2-3	4878.132	4.779	11
(36)	$3^1D - 6^1P^o$	2-1	4526.935	4.420	2

Table 1 -- continued

Mult. No.	Designation	J	λ	log gf	No. Meas.
(37)	$3^1D - 5^1F^o$	2-3	4355.096	4.414	8
(39)	$3^1D - 6^1F^o$	2-3	4108.554	4.110	3
(47)	$4^1P^o - 4p^2\ ^1D$	1-2	5857.454	5.208	12
(48)	$4^1P^o - 6^1S$	1-0	5512.979	4.558	13
(49)	$4^1P^o - 5^1D$	1-2	5188.848	4.979	21

PART TWO

A PRELIMINARY STUDY OF PRESSURE EFFECTS IN ELECTRIC FURNACE SPECTRA.

I. INTRODUCTION

A fundamental problem in the study of solar and stellar atmospheres is the interpretation of the observed spectra in terms of the structure of these atmospheres and the basic physical processes giving rise to line absorption. The method for making such an interpretation is to compute theoretical line profiles and/or curves of growth by using the basic physical data such as f-values and damping constants together with various models for the structure of stellar envelopes. Comparison of the theoretical and observed spectra then suggests the probable physical conditions in the outer layers of the sun and other stars. One such study is currently being carried out by Professors L. Goldberg, L. H. Aller and their colleagues at the University of Michigan.

For complex spectra, experimental measures of f-values and the atomic parameters involved in the calculation of damping constants are to be preferred over the theoretical values. Previous sections of this thesis have dealt with the measurement of relative f-values for neutral calcium lines whereas the following discussion is concerned with a possible laboratory method for measuring damping constants for some absorption lines of astrophysical interest.

A number of studies have already been made on the damping effects in solar and stellar spectra. Among these, the results of Carter[26] revealed an interesting aspect of the general problem. Carter constructed a solar curve of growth for lines of Fe I by using C. W. Allen's equivalent widths and f-values obtained from emission line studies in a King furnace. He found that solar absorption lines arising from states that have odd parity show systematically greater damping

than do those lines arising from levels of even parity. Sandage and Hill[27] discuss similar effects for Cr I lines in the solar spectrum and attribute them to selective pressure broadening in the solar atmosphere. Miss Bell of Harvard[28], in a study based on solar line profiles obtained from the Utrecht Atlas, has also found a parity effect for the Fe I lines and advances arguments to show how this may be explained on the basis of the binding energies of the terms involved in the relevant transitions. Recently, Rogerson[29] has obtained photoelectric solar line profiles, and on the basis of a simplified model for the structure of the sun's atmosphere, he concludes that the solar damping constants are systematically greater for lines of high excitation potentials than for lines of low excitation potentials. However, Miss Bell's results indicate that the solar damping constants are strongly dependent on parity and only weakly on excitation potential, although as Rogerson points out, his observed lines that originate from odd parity levels also have high excitation potentials. The qualitative conclusion to be drawn from the data of these three investigators in that the atomic electrons in the higher energy levels are more loosely bound and are therefore more easily perturbed by colliding particles. These observations may be complicated by the stratified nature of the solar atmosphere, and for this reason, it would be useful to measure damping constants for lines in electric furnace spectra where the temperature, pressure, and relative concentration of atoms are uniform throughout the column of absorbing vapor. Damping data from furnace spectra may then be of considerable assistance in determining the structure of stellar envelopes. The results of Hinnov and

Kohn[30] obtained in emission from flame spectra broadened by molecular nitrogen seem to show binding energy effects similar to those discussed above, but from the standpoint of astrophysical application, it would be better to obtain data from a source like the furnace where line broadening arises from conditions more closely approximating those in stellar atmospheres. Also, much of the existing laboratory data pertain to resonance and low level lines, whereas in future work, an effort should be made to obtain collisional damping constants for the higher level lines of astronomically abundant elements.

It must be emphasized here that the results discussed in the following sections are only tentative and were obtained primarily for the purpose of evaluating a method for experimental measurement of collisional damping constants. Experimental techniques which are more refined than the ones used here will certainly be needed to clarify certain points and some of the possibilities for improving the method will be discussed later. The next section will list some of the theoretical relationships which will be needed to interpret these preliminary data.

II. THEORY

From the point of view of quantum theory, the energy levels of radiating atoms are perturbed by the presence of fields arising from neighboring atoms and ions. The magnitudes of the perturbations depend upon the nature of the interactions and upon the separation of the radiating atom and the perturbing particles. At an infinite separation of the atom and the perturbing particle, the spacings of the energy levels of the atom correspond to the frequencies of the spectral lines emitted or absorbed by the atom in the absence of any perturbations. As the interatomic distance, r, changes, the energy levels of the atom are shifted by the interaction. Usually, the relative spacings of the energy levels and hence the emitted or absorbed frequencies are also functions of r. A group of atoms may radiate at various values of r so that the resulting spectral line is a composite of many sharp lines of slightly differing frequencies. In general, the spectral line so produced will not only be broadened but also will show an asymmetry as well as a shift in its central frequency.

A general theory of pressure* broadening derived on the basis of the above considerations is exceedingly complex, but two asymptotic forms of the theory are usually considered to be adequate for the purposes of astrophysical application. These are frequently referred to as the statistical approximation and as the impact or velocity broadening approximation. Detailed discussions of the general theory of pressure effects are to be found in papers by Margenau and Watson[31], Foley[32], Ch'en and Takeo[33], and Breene.[34] These authors also discuss the limits of validity of the statistical and of the impact

approximations and give extensive bibliographies for both experimental and theoretical work on the subject. The texts by Unsold[3] and by Aller[2] treat those aspects of pressure broadening which are of interest under the conditions prevailing in stellar atmospheres, and the theoretical relationships given below are condensed from their more detailed derivations.

Foley[32] has shown that the impact approximation yields valid results if the effective range of the perturbing forces is negligible in comparison with the average separations of the absorbing atom and the perturbing particles. Under these conditions, the frequency dependence of the atomic absorption coefficient is given by equation 1, page 6. The value of the damping constant is then related to the rate at which line broadening collisions occur. A different frequency dependence of the absorption coefficient results if the effective range of forces is large compared to the average separation of atoms, as is the case when the statistical approximation is valid. Under the conditions prevailing in stellar atmospheres, one or the other of these extremes will usually apply for a given line. The broadening of the hydrogen and helium lines must be treated by the statistical approach whereas that for lines of metals, such as iron and calcium, may be handled by the impact approximation. Therefore, only the results from the impact theory will be of interest in this discussion.

The physical effect of a collision on an emitting atom may, in general, modify the amplitude and/or the phase of the radiated wave. A change in amplitude implies an exchange of kinetic energy between the radiating atom and the perturber and this process would tend to set up

and maintain a condition of thermal equilibrium. For a phase change at constant amplitude, the interaction between the disturbing particle and the radiating atom assumes the form of a time dependent perturbation in the frequency of radiation emitted by the atom. Because of varying spacing of the atomic energy levels with separation of the atom and perturber, the frequency of radiation will vary as the separation changes. For the relatively low pressures in stellar atmospheres, large values of the separation, r, are much more probable than small ones and the shift in frequency of the line will be given by

$$\Delta\nu = Cr^{-n} \quad . \tag{17}$$

In equation 17, n is an integer which is characteristic of the forces between the atom and perturber, and C is a constant which depends on the upper and lower energy levels of the radiating atom. At stellar temperatures, the motion of the perturbing particle relative to the atom may be assumed to be a rectilinear path traversed with the mean relative velocity, V:

$$V = \sqrt{\frac{8RT}{\pi}\left(\frac{1}{M_1} + \frac{1}{M_2}\right)} \tag{18}$$

where R is the gas constant, T is the absolute temperature and M_1 and M_2 are the molecular weights of the atom and perturbing particle. The low densities in stellar atmospheres allow one to neglect multiple collisions. The total phase change of the radiation during a collision is then obtained by integrating equation 17 over the duration of the encounter. This total phase shift, η, is found by assuming the atom to

be at rest and the perturber to be moving past it with velocity V. At time t = 0, let the distance of closest approach be ρ. Defining θ = $\tan^{-1}(Vt/\rho)$, then r = ρ sec θ and

$$\eta = 2\pi \int \Delta\nu \, dt = 2\pi C \int \frac{dt}{(\rho^2 + V^2t^2)^{n/2}} = \frac{2\pi C a_n}{V\rho^{n-1}} \qquad (19)$$

where

$$a_n = \int_{-\pi/2}^{+\pi/2} \cos^{n-2}\theta \, d\theta \quad .$$

The constant, a_n, can be evaluated in terms of the Gamma function. When the phase shift is greater than some critical value, η_o, the emissions before and after the collision may be treated as independent processes in computing the effects on the intensity distribution in the emission line. A Fourier analysis of the wave train then gives an equation for the shape of the line. Since the frequency dependence of the absorption coefficient is the same as the intensity distribution within the corresponding emission line, an equation identical to equation 1 is obtained, except that the damping constant is defined in terms of a collision cross-section. This simplified theoretical treatment accounts for the line broadening but neglects the effects which produce the frequency shift of the line center.

The difficulty with the above approach is the evaluation of the critical phase shift, η_o. Lindhom[35] made a more detailed analysis in which he considered the cumulative effect of many encounters which change the phase by varying amounts. In agreement with the predictions of quantum theory, he found a frequency shift, β, as well as a broadening

so that the absorption coefficient was given by

$$\alpha_\nu = \frac{\pi e^2}{mc} f \frac{\Gamma}{4\pi^2} \frac{1}{(\nu - \nu_o + \beta)^2 + (\Gamma/4\pi)^2} \quad . \tag{20}$$

In practice, there are few collisions where η is large but many where η is small. It is found that those collisions for which $\eta \geq 1$ are the most important in determining the line broadening whereas collisions for which $\eta < 1$ are the more significant for causing line shifts.

Assuming that the phase shifts are produced in accordance with the interaction law given by equation 17, Lindholm's theory yields values of Γ, β, and η_o for different values of n. An interesting result of the theory is that the ratio of broadening to frequency shift, Γ/β, depends only upon the value of n in equation 17. By careful experiments then, it should be possible to determine the interaction law that is effective in broadening a spectral line under given conditions. If the distance of closest encounter, ρ_o, corresponds to a critical phase shift, η_o, then the cross-section for line broadening collisions is $\pi\rho_o^2$, where

$$\rho_o = \left(\frac{2\pi C a_n}{V \eta_o} \right)^{1/(n-1)} \quad .$$

Let N be the number of perturbing particles per cm^3. Then for each radiating atom, the number of broadening collisions per second, Z, is

$$Z = \pi\rho_o^2 VN \quad .$$

The collisional damping constant is related to the collision rate and

is given by

$$\Gamma = 2Z = 2\pi\rho_o^2 VN \quad . \tag{21}$$

The results of the Lindholm theory for the three cases of greatest interest (n = 3,4,6) are summarized in Table 2.

TABLE 2

n	η_o	Γ
3	0.64	$4\pi^3 C_3 N$
4	0.64	$38.8 C_4^{2/3} V^{1/3} N$
6	0.61	$17.0 C_6^{2/5} V^{3/5} N$

Note that for the case n = 3, the damping constant is independent of the relative velocities of the atom and perturber. The physical meaning of the three values of n in Table 2 is, of course, the type of interaction responsible for the perturbation of the atomic energy levels. The case where n = 6 corresponds to a van der Waals type of force between two different neutral atoms, neither of which have a permanent dipole moment; n = 3 is a special case of the van der Waals interaction in which the particles are of the same kind as is the situation for the mutual interaction of calcium atoms. The case where n = 4 is the quadratic Stark effect which arises when neutral elements other than hydrogen and helium are perturbed by ions and electrons.

Stellar atmospheres are composed mainly of hydrogen, a little helium, and very small concentrations of metallic atoms. In those stars

for which the broadening of the spectral lines of neutral metal atoms is relatively large, the concentrations of hydrogen ions and of electrons is considerably less than the concentration of neutral hydrogen atoms. Accordingly, one expects that the main contribution to the pressure broadening of the metallic lines in these stars would arise from the collisions between the atoms and neutral hydrogen atoms. The van der Waals interaction for which n = 6 would apply to such collisions. Calculations based on what is now known about the interaction constants and the physical conditions in stellar atmospheres do, indeed, confirm that most of the broadening may be explained by the van der Waals interaction between the metals and hydrogen. Contributions from the quadratic Stark effect are often significant whereas resonance broadening (the case where n = 3) can usually be ignored in stellar envelopes.

The values of the interaction constants, C_3, C_4 and C_6 must be provided either by quantum mechanical calculation or by laboratory measurements. As is the case with f-values, theoretical calculations of the interaction constants are often difficult to carry out for lines of complex spectra and so experimental procedures should be developed for obtaining such data. Insofar as their effects in broadening the lines of neutral metals is concerned, the noble gases are quite similar to atomic hydrogen and are much more convenient to work with in the laboratory. Thus, in principle, observations on metallic spectral lines broadened by noble gases should be able to supply broadening data of astrophysical interest.

Some experimental work has already been carried out on the broadening of spectral lines by the noble gases, helium, neon and argon. These data are conveniently summarized in an article by Unsold and

Weidmann.[36] The studies were made by a number of workers on the resonance lines of mercury, silver, sodium, potassium, rubidium and cesium. Unsold and Weidmann derived values of C_6 from the experimental measurements and compared these with those calculated on the basis of theory. Except for a few cases, the observed and theoretical values of C_6 generally differed by a factor of two or more. Some of these discrepancies can be explained by the fact that several of the experiments were carried out at high pressures so that the assumption that multiple collisions could be ignored in deriving a value for C_6 was not valid. In those cases where multiple collisions could be ignored, the theoretical and observed interaction constants were in better agreement. Nevertheless, the observed values were generally greater than the theoretical ones and this may mean that the theory for calculating C_6 was inadequate. Further work on other lines and other elements is highly desirable.

By introducing a gas such as helium into a King furnace and studying the broadened absorption lines, one would hope to be able to measure the values of the van der Waals interaction constants, C_6, for lines of neutral metals. Sufficient information on the ionization, electron pressure, and concentration of absorbing atoms in the furnace must be obtained so that the contributions from quadratic Stark effect and resonance broadening may be shown to be negligible in comparison with the van der Waals interactions.

Some of the available relationships for calculating the values of C_3, C_4, and C_6 will now be summarized. The value of C_4 is most easily obtained from laboratory data on the quadratic Stark displacement of spectral lines in a strong electric field. The value of C_4 is given by Aller as

$$C_4 = 6.21 \times 10^{-4} \frac{\overline{\Delta\nu}}{E^2} \quad , \tag{22}$$

where E is the electric field strength in volts per cm, and $\overline{\Delta\nu}$ is the measured displacement in wave numbers of the center of gravity of all the pi and sigma components of the line. The general formulae for C_3 and C_6 can be derived from quantum mechanics by means of perturbation theory. These general equations contain complicated summations involving the absolute f-values of both the perturbing and perturbed atoms, and since many of the f-values are unknown at present, the formulae must be evaluated by approximate methods. The expression for C_3 is given by Unsold as

$$C_3 = \frac{e^2 f}{16\pi^2 m \nu_o} \quad , \tag{23}$$

where e and m are the electronic charge and mass, ν_o and f are the frequency and absolute f-value of the spectral line for which C_3 pertains. For C_6, the general formula of perturbation theory may be simplified if the perturbing particle is a hydrogen or a noble gas atom such as helium or neon. These atoms have an energy gap between the ground state and the first excited state which is large compared to the energy differences between the states of metal atoms so that some of the terms in the general formula may be neglected. The approximate value of C_6 for a given state of the metal atom is then given by Unsold as

$$C_6 = \frac{e^2}{h} \alpha \overline{R^2}$$

where e is the electron charge, h is Planck's constant, α is the polarizability of the perturbing atom, and $\overline{R^2}$ is the mean square radius of the orbit of the excited electron in the metal atom. The polarizability, α, has a value of 6.70×10^{-25} cm^3 for atomic hydrogen and a value of $2.07 \times 10^{-25} cm^3$ for helium. The value of C_6 for a spectral line is found by taking the difference in the C values for the upper (C") and lower (C') states involved in the transition

$$C_6 = C_6'' - C_6' \quad . \tag{25}$$

The values of $\overline{R^2}$ for the different atomic energy levels can be computed from wave functions if these are available. The mean square radius is given by the quantum mechanical formula

$$\overline{R^2} = \int Ur^2 Ur^2 \, dr \tag{26}$$

where U is the normalized radial wave function.

Calculations of R^2 for the hydrogen-like levels of many light atoms may also be made by using the approximate formula

$$\frac{\overline{R^2}}{a_o^2} = \frac{n^{*2}}{2Z^2} \left\{5n^{*2} + 1 - 3\ell(\ell + 1)\right\} \quad . \tag{27}$$

Here a_o is the radius of the first Bohr orbit in hydrogen, n* and ℓ are respectively the effective principal quantum number and the azimuthal quantum number for the energy level under consideration. Z takes the value 1, 2, 3 for neutral, singly and doubly ionized atoms.

Radial wave functions for a few of the states of Ca I have been

given by Hartree and Hartree[24] and more recently by Trefftz.[25] Calculations of $\overline{R^2}$ using these wave functions were made by the author for the $4s^2\ {}^1S$, $4p\ {}^3P^o$, and $4p\ {}^1P^o$ states of Ca I by using Simpson's rule to evaluate the integral in equation 26. For the purposes of comparison, $\overline{R^2}$ values were also calculated from equation 27. The results of these computations are given in Table 3.

TABLE 3

STATE	$\overline{R^2} / a_o^2$		
	Hartree	Trefftz	Equation 27
$4s^2\ {}^1S$	20.6	20.6	12.2
$4p\ {}^3P^o$	29.8	29.8	17.6
$4p\ {}^1P^o$	69.1	63.2	33.3

The values obtained from equation 27 are seen to be in rather poor agreement with those obtained from the wave functions. This is not surprising since these levels of Ca I are not hydrogen-like. The values computed from the two sets of wave functions differ only for the $4p\ {}^1P^o$ state, but since $\overline{R^2}$ is raised to the 0.4 power when calculating damping constants, this difference is not very important for the purposes of the present investigation.

III. OBSERVATIONS

The results reported here were obtained by measuring the equivalent widths of absorption lines which had been broadened by a known pressure of helium gas in the furnace. A curve of growth technique was then used to find the relevant damping constants. Plate calibrations, equivalent widths, and temperatures were obtained by methods which have already been discussed in the section on gf-values. Fine grain, high contrast plates were chosen so that the wings of the broadened absorption lines could easily be observed, since for broadened lines, these wings make important contributions to the equivalent widths. For the purposes of this preliminary study, equivalent width measurements were used since they are more easily and rapidly made than are line profile measurements.

Observations were made on broadened lines of both Fe I and Ca I and will be discussed separately.

A. Results for Fe I

An empirical curve of growth for Fe I was constructed by measuring the equivalent widths from an exposure taken in the second order with the 15-foot spectrograph. The observed furnace temperature was 2448° K and the helium pressure indicated by manometer tubes was 40 cm. The relative gf-values for Fe I lines in this region of the spectrum (λ 3680 - λ 4435) have been measured by King and King[7] and these, together with Boltzmann corrections computed from the observed furnace temperature, were used to calculate the abscissae of the empirical curve. The ordinates were obtained from the measured equivalent widths and the computed Doppler widths. Because relative gf-widths were used, the abscissae are

on an arbitrary scale and a horizontal shift of the empirical curve was made so as to give a reasonable fit to the theoretical curves. The result of this shift is shown in fig. 2 where the abscissae are those pertaining to the theoretical curves. All the observed points can reasonably be represented by a curve of growth with a single damping parameter, $\underline{a}$, having a value of about 0.62. The scatter of the points from this mean curve can be explained as the effect of random errors in equivalent width measurements which are caused by the grain noise of the photographic emulsion. An inspection of fig. 2 shows the scatter is more pronounced for the weaker lines than for the stronger ones and illustrates quite well why a large amount of data is necessary in order to derive reliable relative gf-values from measurements of weak absorption lines. Because of the uncertainties due to the scatter and the graphical method of fitting the points to the theoretical curves, the estimated probable error in the value, $\underline{a} = 0.62$, is about 15%.

The sixty lines used in constructing fig. 2 belonged to ten multiplets of Fe I listed in the Revised Multiplet Table[23] as multiplet numbers, 3, 4, 5, 20, 21, 22, 41, 42, 43 and 45. All the lines arise from the lowest three terms of Fe I , namely a^5D, a^5F, and a^3F, with excitation potentials ranging from 0.0 to 1.6 e.v. The excitation potentials of the upper states involved in the transitions range from 2.9 to 4.8 e.v. Despite the variations in term binding energies, there are no systematic differences in the damping parameter that can be observed in the furnace spectrum. Perhaps this is not surprising since some of these same lines help define the damping portion of the solar Fe I curve of growth, and Carter's results do not seem to indicate systematic damping

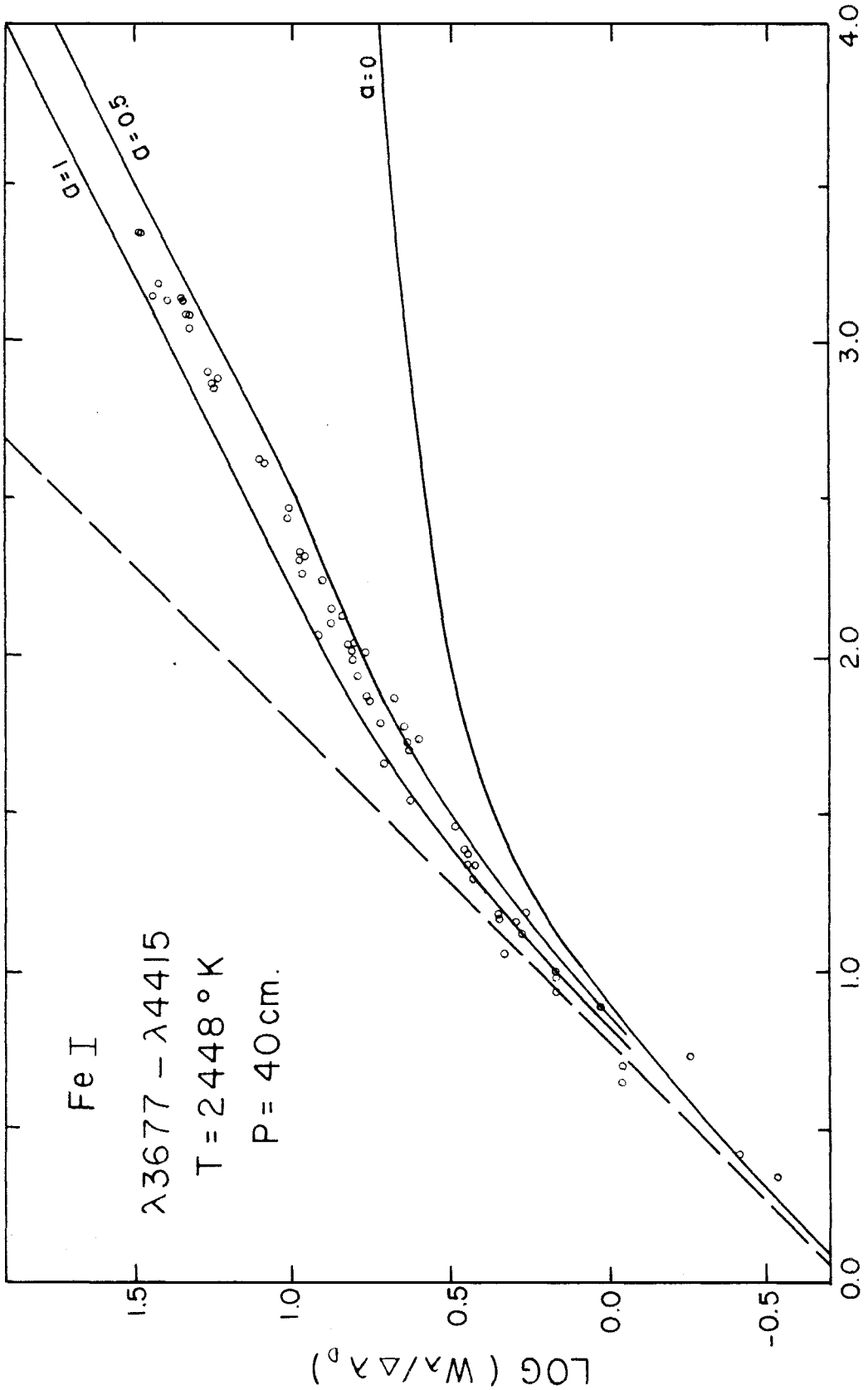
a=1
a=0.5
a=0
Fe I
λ3677 – λ4415
T = 2448° K
P = 40 cm.
LOG (Wλ/Δλ_D)
LOG (Nfh/2 π Δυ_D)
1.5
1.0
0.5
0.0
-0.5
0.0
1.0
2.0
3.0
4.0

FIGURE 2

differences for these multiplets.

An order of magnitude estimate was made for the contribution to the broadening which was due to the mutual collisions of iron atoms. This required an estimate of the concentration of iron atoms in the furnace tube and was carried out as follows: A value of Nfh for one of the lines arising from the ground state was read from the abscissa of fig. 2. Dr. Graydon Bell has recently made an experimental measurement of the absolute f-value for one of the Fe I lines[37] and all King's relative values may now be converted to an absolute scale. This absolute scale was then used to get a value for Nh. The length of the column of absorbing iron vapor, h, was taken to be about eight inches since this is the length of the heated portion of the furnace tube. The result of the calculation showed that the concentration of Fe I atoms in the furnace tube was of the order of 2×10^{14} atoms per cm^3. All the iron lines have absolute f-values which are less than unity, so that an upper limit to the value of C_3 for iron was computed from equation 23 by assuming f = 1. Combining the values of C_3 and N according to the formula given in Table 2 and dividing by $4\pi\Delta\nu_D$ gave $\underline{a} \sim 0.003$ as the upper limit for the contribution from resonance broadening. This is seen to be negligible in comparison with the observed value of $\underline{a} = 0.62$

The estimate for the amount of broadening due to the quadratic Stark effect was more difficult to carry out. Because of their small mass as compared with atomic ions, electrons have high relative velocities and are therefore the most important agents in determining the Stark broadening of a line. No direct information on the electron pressure was obtainable from the iron spectrum, but the order of magnitude

of the electron pressure under furnace conditions was estimated from a calcium spectrum taken at 2500° C and a helium pressure of 20 cm. This was done by measuring the equivalent widths of the resonance lines of both neutral and ionized calcium and using these strengths to derive the relative concentrations of Ca I and Ca II in the furnace tube. Application of the Saha equation showed the electron pressure to be of the order of 10^{-6} atm. Panter and Foster[38] have made laboratory measurements of the quadratic Stark displacement of Fe I lines, but, unfortunately, their data do not pertain to the lines used in this investigation. However, if one may take their values as being representative of the lines observed in the furnace, an $\underline{a}$ value of the order of 0.001 is obtained for the Stark contribution to the broadening. The uncertainties involved in this estimate were large but it would be surprising if the quadratic Stark effect was responsible for more than about 5% of the observed broadening.

The natural broadening arising from the finite lifetimes of excited states could also be neglected in comparison with the observed damping. For lines observed under furnace conditions, natural damping gives an $\underline{a}$ value which is always less than 0.01.

On the basis of the above estimates, it was concluded that the observed value of $\underline{a} = 0.62$ was caused almost entirely by the van der Waals interactions between iron and helium atoms. Hence, $\underline{a} = 0.62$ corresponds to a mean value of $C_6 = 4.2 \times 10^{-32}$ for these lines; for collisions between iron and hydrogen atoms, the value of C_6 would be 14×10^{-32}.

It is interesting to apply this result to the solar spectrum.

The temperature and pressure at an optical depth in the continuum of 0.5 may be taken as the appropriate physical conditions under which these iron lines are formed in the sun. At an optical depth of 0.5, a theoretical solar model calculated by Munch[39] gives T = 5563° K and log P = 4.82, where P is the gas pressure in dynes per cm^2. A calculation using these T and P values together with $C_6 = 14 \times 10^{-32}$ yielded a value for the solar damping parameter of $\underline{a} = 0.069$. The contribution from quadratic Stark broadening was estimated to be of the order of 0.01. This gives a total damping of $\underline{a} = 0.08$, and is in excellent agreement with the results of Miss Bell's curve of growth studies in which she also obtained a value of 0.08 for these iron lines.

B. Results for Ca I

By using the relative gf-values in Table 1, empirical curves of growth were constructed for the calcium lines in the wavelength region λ 5000 Å - λ 6750 Å. The equivalent widths were obtained from plates taken in the first order with the 15-foot spectrograph. The method for fitting the observed points to the theoretical curves was the same as that discussed in Part A above. The results are shown in figs. 3 and 4 where different symbols are used to distinguish the various low terms from which the absorption lines arise. The temperature and pressure pertaining to fig. 3 were 2139° K and 35 cm., whereas those for fig. 4 were 2926° K and 5 cm. The results obtained from a plate taken at 2400° K and 35 cm., (not shown) were very similar to those given by fig. 3. The lines used are listed in the Revised Multiplet Table as belonging to multiplet numbers 1, 3, 18, 19, 20, 21, 22, 33, 34, 47, 48 and 49. One line from the ground state, λ 6572 $4^1S_o - 4^3P_1{}^o$, is included. The rest

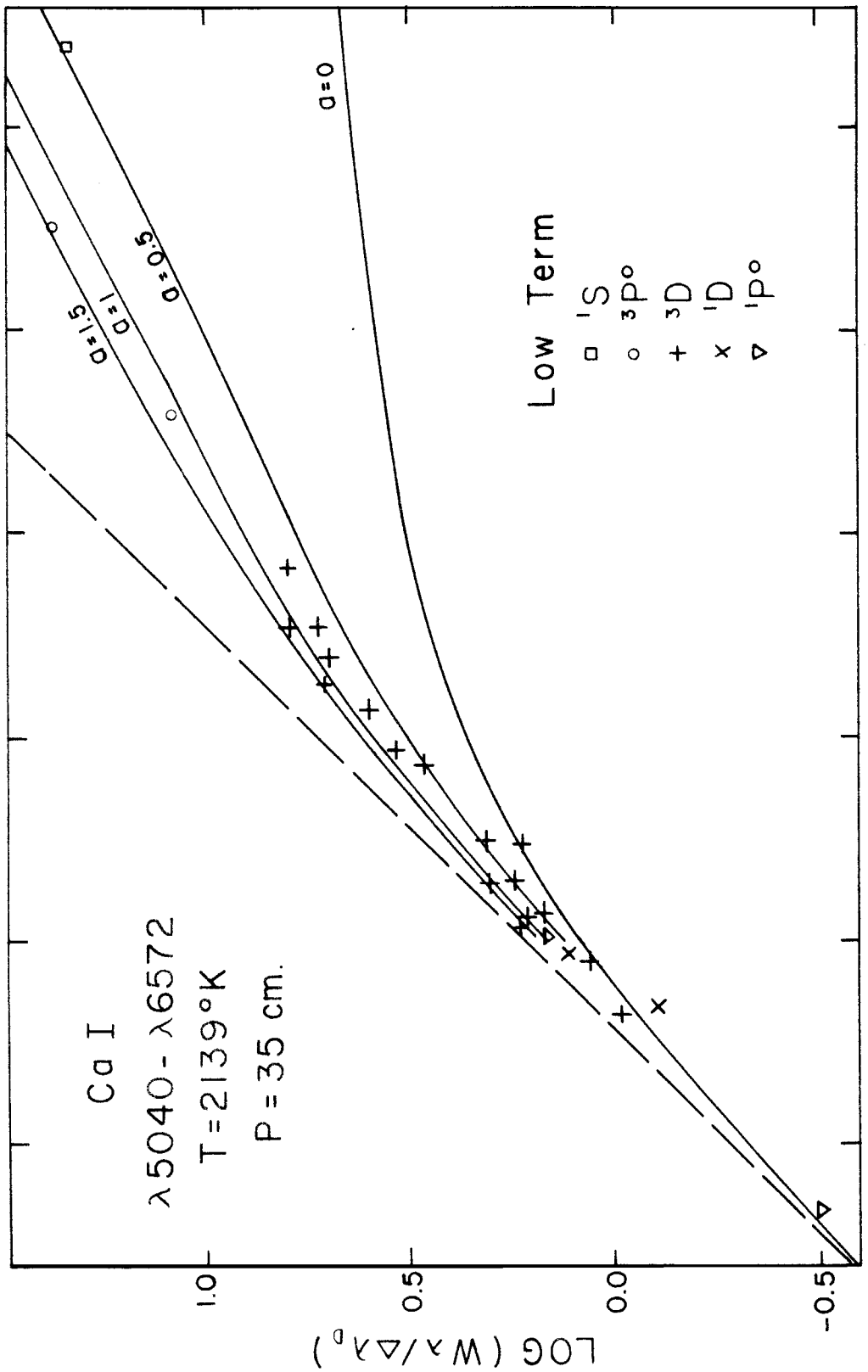
Ca I
λ5040 - λ6572
T = 2139°K
P = 35 cm.
a=0
a=0.5
a=1
a=1.5
Low Term
□ ¹S
○ ³P°
+ ³D
× ¹D
▽ ¹P°
LOG (Wλ/Δλ_D)
LOG (Nfh/2πΔν_D)
-0.5
0.0
0.5
1.0
0.5
1.0
1.5
2.0
2.5
3.0

FIGURE 3

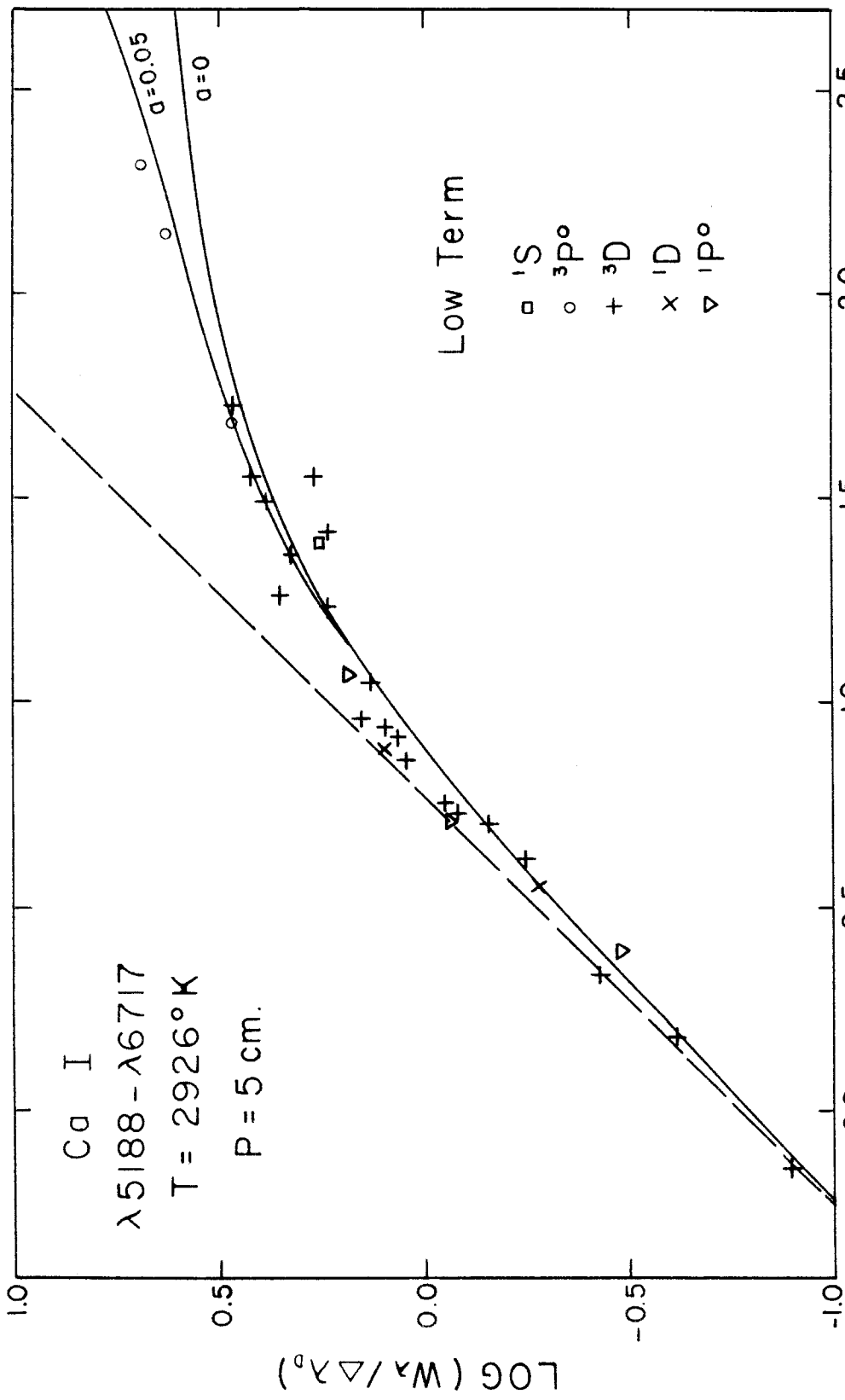
Ca I
λ5188-λ6717
T = 2926° K
P = 5 cm.
a=0.05
a=0
Low Term
□ ¹S
○ ³P°
+ ³D
× ¹D
▽ ¹P°
LOG (Wλ/Δλ_D)
LOG (Nfh/2πΔν_D)
1.0
0.5
0.0
-0.5
-1.0
0.0
0.5
1.0
1.5
2.0
2.5

FIGURE 4

are lines arising from terms whose low excitation potentials range from 1.9 to 2.9 e.v. The effect of the difference in pressure is immediately obvious when one compares the two figures. The spectral lines in fig. 3 show much greater damping than do those in fig. 4.

As is seen from the points in fig. 3, lines arising from terms of high excitation potential show a damping parameter which is two to three times greater than that of the ground state line λ 6572. It is doubtful if this effect is caused by systematic errors in the gf-values since these were determined from a large number of measurements on weak lines. The estimated probable errors are about 15% for the gf-values whereas those for the equivalent widths used in figs. 3 and 4 may be as large as 25%. It seems most likely that the effect is due to a selective pressure broadening similar to that observed in the solar spectrum by Carter, Bell and Rogerson.

Attempts were made to compare the observed values of the damping parameter with those calculated from theory. Unfortunately, the values for the van der Waals contribution to the damping constant could be calculated only for the two lines arising from the ground state, λ 6572 $4^1S_o - 4^3P_1^o$, and λ 4226 $4^1S_o - 4^1P_1^o$, since the results obtained in Table 3 indicate that the hydrogenic approximation may not be reliable for the higher Ca I states. The resonance line, λ 4226, is not included in the observations plotted in figs. 3 and 4, but data pertaining to it will be presented later. For a temperature of 2139° K and a helium pressure of 35 cm., the van der Waals component of the damping parameter should have a value of 0.26, whereas the value observed from fig. 3 is greater than this by almost a factor of two. Jenckel and Kopfermann[40]

found a value of $\Delta\overline{\nu} = 0.008$ cm^{-1} for the Stark displacement of the resonance line, λ 4226, in a field of 200,000 volts per cm., and if this may be taken as representative of the other lines, the Stark component should give an $\underline{a}$ value of the order of 10^{-4} or 10^{-5}, which is negligible in comparison with the observed values.

The contribution arising from resonance broadening was calculated in a manner similar to that already described for iron. The results indicate that resonance broadening should be negligible (i.e. $\underline{a} \sim 10^{-5}$) for the intersystem line, λ 6572, but $\underline{a}$ may be of the order of 0.1 for the other lines plotted in fig. 3. For the resonance line, λ 4226, the contribution of resonance broadening was found to be of the order of 0.4. All these calculations were made by assuming Trefftz's[25] value of 1.46 for the absolute f-value of λ 4226 together with Prokofjew's[13] value of 3.3×10^4 for the ratio of the f-values of λ 4226 and λ 6572.

For the lines plotted in fig. 3, the estimated theoretical $\underline{a}$ values associated with the various sources of broadening are summarized in Table 4. The observed values from fig. 3 are also given for comparison.

TABLE 4

Source	Intersystem line λ 6572	High level lines
Van der Waals broadening	$\underline{a} = 0.26$	$\underline{a} > 0.26$ (?)
Stark broadening	$\underline{a} \sim 0.0001$	$\underline{a} \sim 0.0001$
Resonance broadening	$\underline{a} \sim 0.00001$	$\underline{a} \sim 0.1$
Natural broadening	$\underline{a} < 0.01$	$\underline{a} < 0.01$
Total from estimates	$\underline{a} = 0.26$	$\underline{a} > 0.36$ (?)
Observed from fig. 3	$\underline{a} \simeq 0.5$	$\underline{a} \simeq 0.7$ to 1.5

Thus, the observed damping was found to be larger than that which could be accounted for by the theoretical estimates. Calculations for the lines plotted in fig. 4 indicated a similar discrepancy between observation and theory. For the intersystem line, at least, the approximate theory which was used to calculate the van der Waals interaction constant from the wave functions would, therefore, seem to be inadequate. In view of the large uncertainties in the estimate for the resonance interaction, it appears likely that resonance broadening may have contributed an appreciable fraction of the broadening observed for the high level lines.

Further evidence for a fairly large resonance broadening contribution was obtained by studying λ 4226 and λ 6572 on plates taken with a concave grating spectrograph of one meter focal length. It was necessary to use this lower dispersion instrument to obtain simultaneous photographs of λ 4226 and λ 6572, since for a given setting, the 15-foot spectrograph covered a wavelength interval of only 1700 Å in the first order. In conjunction with the one meter spectrograph, a 4 filament projection bulb operated at 30 to 33 amperes d.c. was used as the source of the continuous spectrum. A large sample of calcium was placed in the furnace tube so that both lines were strong enough to be observed in the square root region of the curves of growth. The equivalent widths were measured and their ratio then gave estimates for the ratio of $\sqrt{f\Gamma}$ for the two lines. The equivalent width of the resonance line was extremely large, being as much as 60 or 70 Angstroms, whereas that of λ 6572 was of the order of a fraction of an Angstrom. The large equivalent width of λ 4226 was difficult to measure because of the wavelength variation of the plate sensitivity over the region of interest. Several different types of plates were tested and it was found that all showed some degree

of sensitivity variation over the wavelength interval λ 3800 - λ 4600. Since the very extended wings of λ 4226 gave large contributions to the equivalent width, the following procedure was used to determine the continuum level on the microphotometer tracings: With the furnace in operation, a photograph was taken which showed the lines in absorption. The furnace tube then was rapidly cooled by shutting off the furnace power and a second exposure showed only the continuum. The fluctuations due to grain noise appeared on the microphotometer tracings so that there was still some uncertainty as to the wing variation at large distances from the line center. The measured equivalent widths of λ 4226 were felt to be lower limits since there is a tendency to underestimate the contributions from the far wings of a very strong line.

As has been stated, the method used gave values of the ratio of $\sqrt{f\Gamma}$ for λ 4226 and λ 6572. Prokofjew's value of 3.3×10^4 was assumed to be correct for the ratio of the f-values of λ 4226 and λ 6572, and using this then gave Γ(4226)/ Γ(6572). This ratio was found to be from two to three times greater than the value obtained on the assumption that the broadening of both lines was caused only by van der Waals interactions with helium atoms as calculated from the data given in Table 3. According to equation 23, the resonance broadening is proportional to the f-value of the line so that at least some of the observed discrepancy was tentatively interpreted as being due to a large resonance contribution to the broadening of λ 4226.

Clearly, additional observations on the calcium lines using more refined techniques will be required before the relative importance of the different broadening mechanisms can be more completely understood.

IV. SUGGESTIONS FOR FURTHER RESEARCH

Although the observations of the calcium spectra discussed above are, at present, difficult to interpret with any degree of certainty, the results derived for iron would seem to indicate that line broadening studies using a King furnace are able to provide astrophysically important data on van der Waals interaction constants for neutral metal atoms. This section will be devoted to a discussion of some possible ways in which the reliability and the accuracy of such measurements may be improved.

The contributions of quadratic Stark effect seem to be negligible for the two elements studied here, but for lines of other elements, a more complete study of the ionization and electron pressure in the furnace may be required. In addition, more data on the Stark interaction constants are needed. These could be most suitably supplied by laboratory measurements of line displacement in large electric fields and by shock-tube studies.

One of the sources of greatest uncertainty in the data discussed in section III was the possibility that resonance broadening contributed significantly to the observed collisional damping constants. Contributions from this source of broadening could be considerably reduced by using very small concentrations of absorbing vapor in the furnace tube. In order to observe strong absorption lines formed by relatively small concentrations of atoms, extremely long absorbing path lengths would be required. Long path lengths are most easily obtained with an apparatus in which the light beam is made to undergo multiple traversals in the absorbing vapor. This is done by means of successive reflections from a system of mirrors and one such instrument has been described by

Bernstein and Hertzberg.[41]

It will be noted that the curve of growth method employed here to study damping constants required the use of relative f-values. The accuracy of the results, therefore, is limited by the accuracy of the relative f-values. It would be highly desirable to have a method for measuring damping constants which is independent of f-values. A possible way in which this might be done is to use a multiple traversal apparatus in which the path length could be changed in a known manner during a sequence of exposures. However, there would be two difficulties in using such a technique. First, a very large range in the number of traversals would be needed to observe a given line at several points in the linear as well as in the square-root regions of the curves of growth. Each succeeding traversal would require two additional reflections and, since light losses occur with each reflection, the intensity of the emergent beam after a large number of traversals would be considerably reduced over that from a few traversals. This would mean that the exposure times for the longer path lengths would be considerably greater than for the shorter ones. Second, the number of absorbing atoms in the furnace tube may change during the time required to make several different settings of the path length. This would be an especially serious problem when studying elements such as calcium, where, with the same furnace temperature, the concentration of absorbing atoms can be observed to decrease by as much as a factor of two within a period of five minutes. Thus, it would seem to be better to use a method in which the number of traversals could be left unchanged for observations on a given set of lines.

More attention should also be given to the methods for observing the lines with the spectrograph. The errors in equivalent width measurements due to the grain noise of the photographic emulsion need to be considerably reduced. Perhaps the best way to achieve this is to discard photographic photometry completely and to develop a photoelectric apparatus for measuring the absorption lines. Equivalent widths obscure a great deal of information and it is worthwhile to consider instead the possibility of measuring line profiles. If the instrumental profile is accurately determined, true line profiles may be obtained, and these may be made to yield values of the damping constants independent of the knowledge of the f-values. An example of such a technique is the study of the solar lines made by Rogerson.[29] A photoelectric method for studying line profiles would require that the number of absorbing atoms in the furnace tube remain constant while the profile is being scanned, but at least for studies on elements such as iron, an apparatus could probably be constructed which would be fast enough to overcome this difficulty.

On the basis of this discussion, the best method for measuring collisional damping parameters would seem to require the following techniques:

1. The use of low densities of absorbing atoms in the furnace tube together with a fixed multiple traversal apparatus to obtain long path lengths.
2. The use of a rapid photoelectric method for scanning absorption line profiles.

In addition, valuable supplementary data could also be obtained if line

shifts could be measured by means of interferometric techniques, since the results of the Lindholm theory indicate that the ratio of broadening to shift, Γ/β, should be constant for a given line. If this is confirmed by detailed observations on several lines of a given spectrum, line shift measurements may, in fact, prove to be the most rapid way of obtaining damping data for the other lines of the spectrum.

The tentative procedure outlined above would require a considerable amount of time and instrumentation, and it is hoped that this discussion will provide some basis for further research on the possibilities for measuring collisional damping parameters for lines of astrophysical interest.

REFERENCES

(1) E. U. Condon and G. H. Shortley, The Theory of Atomic Spectra, Cambridge University Press, Cambridge (1935)

(2) L. H. Aller, Astrophysics; The Atmospheres of the Sun and Stars, Ronald Press, New York (1953)

(3) A. Unsold, Physik der Sternatmospharen, 2nd ed., Springer-Verlag, Berlin (1955)

(4) A. C. G. Mitchell and M. W. Zemansky, Resonance Radiation and Excited Atoms, Cambridge University Press, Cambridge (1934)

(5) S. A. Korff and G. Breit, Revs. Modern Phys. 4, 471-503 (1932)

(6) R. B. King and A. S. King, Astrophys. J. 82, 377-395 (1935)

(7) R. B. King and A. S. King, Astrophys. J. 87, 24-39 (1938)

(8) R. B. King, Astrophys. J. 94, 27-29 (1941)

(9) R. B. King, Astrophys. J. 105, 376-389 (1947)

(10) R. B. King, Astrophys. J. 108, 87-91 (1948)

(11) A. J. Hill and R. B. King, J. Opt. Soc. Am. 41, 315-321 (1951)

(12) R. B. King, B. R. Parnes, M. H. Davis and K. H. Olsen, J. Opt. Soc. Am. 45, 350-353 (1955)

(13) W. Prokofjew, Z. Physik 50, 701-715 (1928)

(14) E. Katz and L. S. Ornstein, Physica 4, 757-760 (1937)

(15) J. W. Schuttevaer, M. J. de Bont and Th. H. van den Broek, Physica 10, 544-552 (1943)

(16) L. C. Green, Proceedings of the N. S. F. Conference on Stellar Atmospheres, 72-79, Indiana University (1954)

(17) S. S. Penner and R. W. Kavanagh, J. Opt. Soc. Am. 43, 385-388 (1953)

(18) F. Hjerting, Astrophys. J. 88, 508-515 (1938)

(19) D. L. Harris, Astrophys. J. 108, 112-115 (1948)

(20) C. E. Moore, Atomic Energy Levels - Vol. 1, National Bureau of Standards Circular 467, Washington (1949)

(21) A. J. Hill, Thesis, Calif. Inst. of Tech. (1950)

(22) A. S. King, Astrophys. J. 56, 318-339 (1922)

(23) C. E. Moore, A Multiplet Table of Astrophysical Interest, Contributions from the Princeton University Observatory No. 20, Princeton (1945)

(24) D. R. Hartree and W. Hartree, Proc. Roy. Soc. (London) A 164, 167-191 (1938)

(25) E. Trefftz, Z. Astrophys. 29, 287-303 (1951)

(26) W. W. Carter, Phys. Rev. 76, 962-966 (1949)

(27) A. Sandage and A. J. Hill, Astrophys. J. 113, 525-530 (1951)

(28) B. Bell, A Study of Doppler and Damping Effects in the Solar Atmosphere, Harvard Special Report No. 35 (1951)

(29) J. B. Rogerson, Jr., Astrophys. J. 125, 275-284 (1957)

(30) E. Hinnov and H. Kohn, J. Opt. Soc. Am. 47, 156-162 (1957)

(31) H. Margenau and W. W. Watson, Revs. Modern Phys. 8, 22-53 (1936)

(32) H. M. Foley, Phys. Rev. 69, 616-628 (1946)

(33) S. Ch'en and M. Takeo, Revs. Modern Phys. 29, 20-73 (1957)

(34) R. G. Breen, Jr., Revs. Modern Phys. 29, 94-143 (1957)

(35) E. Lindholm, Arkiv Mat. Astron. Fysik 28B, No. 3 (1942); Arkiv Mat. Astron. Fysik 32A, No. 17 (1946)

(36) A. Unsold and V. Weidmann, Vistas in Astronomy - Vol. 1, 249-256, Pergamon Press, London (1955)

(37) G. D. Bell, Thesis, Calif. Inst. of Tech. (1957)

(38) F. S. Panter and J. S. Foster, Proc. Roy. Soc. (London) A 162, 336-348 (1937)

(39) G. Munch, Astrophys. J. 106, 217-223 (1947)

(40) L. Jenckel and H. Kopfermann, Z. Physik 117, 145-155 (1941)

(41) H. J. Bernstein and G. Hertzberg, J. Chem. Phys. 16, 30-39 (1948)